

### Noise-induced escape from attractors in one-dimensional maps

Paul D. Beale

*Department of Physics, University of Colorado at Boulder, Boulder, Colorado 80309*

(Received 24 February 1989)

The addition of external noise to a dynamical system described by an iterated map causes the orbit to escape from the attractor. The escape time  $\tau$  has the behavior  $\tau \approx \tau_0 \exp(E_0/\Gamma)$ , where  $\Gamma$  is the noise temperature,  $E_0$  is the minimum escape energy, and  $\tau_0$  is the inverse of the attempt rate. We will describe an analytical method for calculating the mean escape time based on the principle of minimum escape energy. Analytical solutions for  $E_0$  are presented for values of the mapping control parameter  $a$  close to tangent bifurcations and interior crises. The minimum escape energy displays a power-law dependence on the control parameter near tangent bifurcations ( $E_0 \sim |a - a_t|^{3/2}$ ) and near interior crises ( $E_0 \sim |a - a_c|^2$ ). Numerical solutions are given for control-parameter values throughout the range of the attractor. The results agree with the results of Monte Carlo simulations of the logistic map and with independent work on the noise stability of rf-driven Josephson junctions.

Recent work<sup>1-4</sup> on the stability of rf-driven Josephson junctions to the addition of thermal noise indicates that the escape time from a phase-locked attractor increases exponentially as the inverse of noise temperature in the circuit.<sup>5</sup> This is explained in terms of the minimum escape energy from the attractor and a prescription is given for the calculation of that escape energy.<sup>3,4</sup> A large literature exists for the calculation of the thermal escape rate from local minima of the potential energy.<sup>6</sup> The difference here is that the escape is from the attractor of a dynamical system and not from a minimum in the potential energy. However, it has been shown,<sup>1,4,5</sup> that this escape rate is characterized by a definite minimum escape energy.

The attractor of the rf-driven Josephson equation<sup>7,8</sup> has been mapped by a number of authors.<sup>1,2,9,10</sup> Numerical studies<sup>1,2</sup> in which white noise is added to the rf-driven Josephson equation indicate that the escape energy tends to zero at both ends of the stability range of periodic attractors. The periodic attractors are bounded by a tangent bifurcation and an interior crisis as the control parameter is varied. Because of the highly nonlinear form of the Josephson equation in the region of the attractors of interest, it is difficult to give analytical arguments for the behavior of the minimum escape energy as a function of the control parameter.

This difficulty can be overcome by the study of a simpler dynamical system which exhibits the same qualitative behavior.<sup>11-13</sup> Universality arguments can then be applied to extend the results to other systems. In the absence of noise and in the parameter range near phase-locked attractors the resistively shunted Josephson equation<sup>7,8</sup> exhibits<sup>1,2</sup> a tangent bifurcation<sup>14,15</sup> to a period one solution, a series of period doubling bifurcations to a strange attractor,<sup>12,13</sup> and, finally, an interior crisis<sup>16</sup> at which the phase lock is lost. With the addition of a small amount of additive noise, the escape time (the average time for the system to lose phase lock)  $\tau$  is of the form<sup>1-5</sup>

$$\tau \approx \tau_0 \exp(E_0/\Gamma) \tag{1}$$

where  $\Gamma$  is the noise temperature and  $E_0$  is the minimum escape energy. We will demonstrate that for the logistic map<sup>11-13</sup> the minimum escape energy is nonzero throughout the attracting region and tends to zero at the tangent bifurcation and the crisis. Also, the minimum escape energy is largest roughly in the middle of the one-cycle region. The point of maximal minimum escape energy is interesting for applications because it is the point where the system is most stable to the addition of thermal noise.

The model we will use has the same qualitative features as the driven Josephson junction. For simplicity we chose the logistic map<sup>11-13</sup> plus additive noise.<sup>15,17</sup> The dynamics are given by

$$x_{n+1} = f(x_n) + \xi_n \tag{2}$$

where  $f$  is the logistic map<sup>11-13</sup>

$$f(x) = a - x^2 \tag{3}$$

and the noise term is Gaussian white noise

$$\langle \xi_n \xi_{n'} \rangle = \Gamma \delta_{n,n'} \tag{4}$$

The brackets denote a statistical average,  $\Gamma$  is the noise temperature, and  $\delta_{n,n'}$  is the Kronecker delta. In the absence of noise ( $\Gamma=0$ ) the map exhibits a single attractor<sup>11,12</sup> for each  $a$  in the range  $-\frac{1}{4} \leq a \leq 2$ . The tangent bifurcation<sup>14,15</sup> to a one-cycle occurs at  $a = a_t = -\frac{1}{4}$ , the one-cycle is superstable at  $a=0$ , a pitchfork bifurcation from the one-cycle to a two-cycle occurs at  $a=0.75$ , the two-cycle is superstable at  $a=1$ , the Feigenbaum chaotic attractor<sup>12,13</sup> appears at  $a=1.401155$ , the superstable three-cycle is at  $a=1.754877666$ , and the interior crisis<sup>16</sup> is at  $a = a_c = 2$ . A plot of the attractor as a function of  $a$  is shown in Fig. 1. One might note the similarity between the attractor in Fig. 1 and the attractor in Fig.

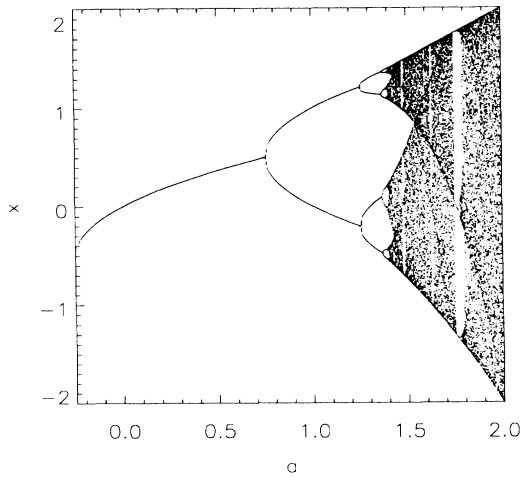


FIG. 1. The attractor for the logistic map (3) in the absence of noise. All variables plotted in this and all of the remaining figures are dimensionless.

1(b) of Ref. 1.

When noise is added to the mapping<sup>15,17</sup> the orbit will eventually escape from the attractor<sup>18-20</sup> ( $|x| < \frac{1}{2}[1 + (1+4a)^{1/2}]$ ). The escape rate can be determined by the following argument based on the minimum escape energy technique.<sup>4</sup> The rate of escape is given by

$$R = \sum_{\substack{\text{paths of} \\ \text{length } N}} \sum_{N=0}^{\infty} P_N, \quad (5)$$

where the sum is over all independent paths that begin on the attractor and end on the boundary of the basin of attraction at the unstable fixed point  $x^* = -\frac{1}{2}[1 + (1+4a)^{1/2}]$ , and  $P_N$  is the probability that a given path of  $N$  steps can occur. This probability is given by

$$P_N = (2\pi\Gamma)^{-N/2} \exp\left[-\frac{1}{2\Gamma} \sum_{n=0}^{N-1} \xi_n^2\right] \quad (6)$$

since the noise terms are uncorrelated and have a Gaussian distribution with width  $\Gamma^{1/2}$ . In the limit of small noise temperature the rate will be dominated by the path which has the highest probability. We can define the noise energy for a given escape path by

$$E = \frac{1}{2} \sum_{n=0}^{N-1} \xi_n^2 = \frac{1}{2} \sum_{n=0}^{N-1} [x_{n+1} - f(x_n)]^2 \quad (7)$$

where  $x_0$  is on the attractor and  $x_N = x^*$ , where  $x^*$  is the boundary of the basin of attraction of the map. The most probable escape path is the one in which  $E$  is minimized over all possible paths. The value of  $E$  on this path is the minimum escape energy  $E_0$ . The escape rate will be dominated by this path so as to give

$$R \approx \frac{1}{\tau_0} \exp(-E_0/\Gamma). \quad (8)$$

The escape time  $\tau = 1/R$  is then given by the general re-

sult shown in Eq. (1). The validity of Eq. (1) is demonstrated in Fig. 2 using Monte Carlo results described below. The average of the logarithm of the escape time is shown versus  $1/\Gamma$ . The slope of the line is the minimum escape energy  $E_0$  for this value of the control parameter  $a$ . The prefactor  $\tau_0$ , the time between attempts or the inverse of the attempt rate, is proportional to the number of paths close to the path with minimum escape energy.

The method for calculating the minimum escape energy is the following. In Eq. (7) let  $x_n \rightarrow x_n + \eta_n$  where  $\eta_n$  is an arbitrary small variation. The boundary conditions on  $\eta_n$  are  $\eta_0 = 0$  and  $\eta_N = 0$ . All the remaining  $\eta_n$ 's are arbitrary. The approach is to find paths in which the escape energy is extremal with respect to variations in the  $\eta_n$ 's. We have

$$E \rightarrow E + \delta E \quad (9)$$

where

$$\delta E = \sum_{n=0}^{N-1} [x_{n+1} - f(x_n)][\eta_{n+1} - f'(x_n)\eta_n] + O(\eta^2). \quad (10)$$

The function  $f'(x)$  is the first derivative of  $f(x)$ . By relabeling the terms proportional to  $\eta_n$  ( $\eta_n \rightarrow \eta_{n+1}$ ), Eq. (10) can be rewritten as

$$\delta E = \sum_{n=0}^{N-1} \{x_{n+1} - f(x_n) - [x_{n+2} - f(x_{n+1})]f'(x_{n+1})\} \\ \times \eta_{n+1} + [x_{N+1} - f(x_N)]f'(x_N)\eta_N \\ - [x_1 - f(x_0)]f'(x_0)\eta_0 + O(\eta^2). \quad (11)$$

The terms outside the summation vanish because of the boundary conditions. The function in the curly brackets

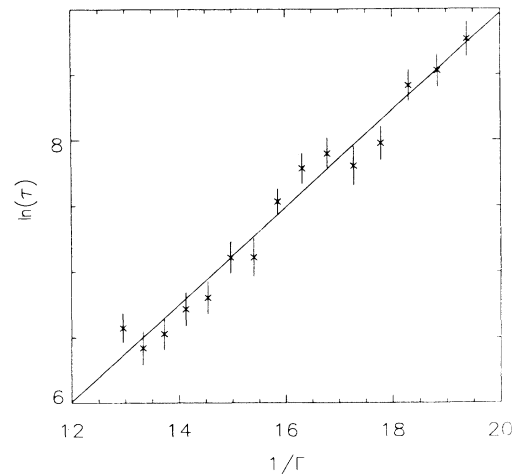


FIG. 2. The logarithm of the escape time vs  $1/\Gamma$  for  $a=0.50$ . The line is a fit to the data indicating that Eq. (1) is valid. The fit gives  $E_0 = 0.371 \pm 0.016$  and  $\ln(\tau_0) = 1.563 \pm 0.258$ .

inside the summation must vanish for every term. The equation of motion for an extremal path is then given by

$$x_{n+2} = f(x_{n+1}) + \frac{1}{f'(x_{n+1})} [x_{n+1} - f(x_n)] . \quad (12)$$

Note that a given point in the extremal trajectory  $x_n$  depends on the *two* previous values,  $x_{n-1}$  and  $x_{n-2}$ . It is necessary to start the motion along the extremal path in the following manner. The first value,  $x_0$ , must be an element of the attractor since the orbit starts on the attractor prior to the addition of the noise. The second element is given by  $x_1 = f(x_0) + \xi_0$ . The remaining points in the orbit are determined by (12). The orbit is followed until  $x_n$  is outside the basin of the attractor,  $|x_n| \geq |x^*|$ . The minimization procedure is carried out by minimizing the energy given by Eq. (7) over all values of  $\xi_0$  and all elements of the attractor.

It is interesting to note the similarity of this result to Kautz's results as the minimum noise energy method is applied to a second-order differential equation. He finds<sup>4</sup> that the escape path with minimum noise energy is described by a fourth-order differential equation with boundary conditions that the path begins on the attractor and ends on the boundary of the basin of attraction.

Equation (12) cannot be solved analytically in general even for the logistic map. However, analytical solutions can be found when the control parameter  $a$  is close to the tangent bifurcation point ( $a_t = -\frac{1}{4}$ ) or close to the crisis point ( $a_c = 2$ ).

Near the tangent bifurcation it is possible to expand Eq. (12) in terms of the small parameter  $a - a_t$ . In that limit Eq. (12) becomes

$$y_{n+2} - 2y_{n+1} + y_n = -2(a - a_t)y_{n+1} + 2y_{n+1}^3 + O((a - a_t)^2) , \quad (13)$$

where  $y_n = x_n + \frac{1}{2}$ , the initial value for  $y$  is the one-cycle attractor  $y_{-\infty} = (a - a_t)^{1/2}$ , and the final value is  $y_{\infty} = -(a - a_t)^{1/2}$ . For  $a - a_t$  sufficiently small, Eq. (13) can then be written as a differential equation

$$\frac{d^2y}{dn^2} = -2(a - a_t)y + 2y^3 . \quad (14)$$

This is possible because in the limit of small  $a - a_t$   $y_n$  is a slowly varying function of  $n$ . The solution of (14) is

$$y_n = (a - a_t)^{1/2} \tanh[(a - a_t)^{1/2} n] , \quad (15)$$

and the minimum escape energy (7) is given by

$$E_0 = \frac{8}{3}(a - a_t)^{3/2} . \quad (16)$$

The minimum escape energy tends to zero as  $a \rightarrow a_t$ . This result scales in the same manner as the results for the laminar flow time for intermittency plus noise just on the other side of the tangent bifurcation. That theory<sup>15</sup> predicts that the laminar flow time for  $a$  just beyond the tangent bifurcation scales with the variable  $(|a - a_t|^{3/2})/\Gamma$  which is also what we observe on the stable side of the tangent bifurcation.

The escape energy for the resistively shunted Josephson equation also tends to zero at the tangent bifurcation. A calculation based on the Fokker-Planck equation<sup>10</sup> [see Eq. (12) of Ref. 1] also predicts the dependence  $E_0 \approx |a - a_t|^{3/2}$ . Based on these two results we conjecture that the exponent  $\frac{3}{2}$  is universal for escape from attractors close to tangent bifurcations. The prefactor in (16) is nonuniversal.

At the other end of the attracting range the system has an interior crisis. The small parameter in this case is  $a - a_c$ . The crisis is caused by the critical point  $x = 0$  being mapped onto the boundary of the attractor  $x^*$  in two iterations of the map. For most of the parameter values near  $a = a_c = 2$  the attractor is chaotic and the distribution of  $x^*$  on the attractor is continuous. When  $a \simeq a_c$  the escape path with minimum noise energy is

$$\begin{aligned} x_0 &= 0 , \\ x_1 &= 2 - (a_c - a) + \xi_0 , \\ x_2 &= -2 + 3(a_c - a) - \frac{17}{4}\xi_0 + O((a_c - a)^2) , \\ &\dots \end{aligned} \quad (17)$$

where

$$\xi_0 = \frac{5}{8}(a_c - a) . \quad (18)$$

This particular choice of  $\xi_0$  gives a geometric approach to the unstable fixed point at  $x^* = -2 + \frac{1}{3}(a_c - a) + O((a_c - a)^2)$ . We have

$$(x_n - x^*) \approx (x_{n-1} - x^*) / [4 - \frac{2}{3}(a_c - a)] \text{ for } n > 2 . \quad (19)$$

The escape energy for this path is obtained by summing Eq. (7) exactly using Eqs. (17-19):

$$E_0 \approx \frac{5}{24}(a_c - a)^2 . \quad (20)$$

The minimum escape energy vanishes quadratically in  $a_c - a$  as  $a \rightarrow a_c$ . Arcelli *et al.*<sup>18</sup> and Takesue and Kaneko<sup>19</sup> also predict that  $E_0$  tends to zero quadratically as  $a \rightarrow a_c$  but with a different prefactor.

Similar behavior was observed in the resistively shunted Josephson equation. Kautz's numerical results<sup>1,2</sup> give a dependence  $E_0 \sim (a_c - a)^{1.8}$  but with no estimate of the statistical error of the exponent. Based on the similar behavior of these different systems we conjecture that  $E_0$  always will tend to zero quadratically as  $a \rightarrow a_c$  for any system which exhibits an internal crisis. The prefactor in (20) is, of course, nonuniversal.

For other values of the control parameter one must resort to numerical techniques in which a search is conducted for the path which satisfies (12) and has minimum energy (7). This is easily done for the low-order periodic orbits. One merely sets  $x_0$  to be an element of the attractor and varies  $\xi_0$  numerically so as to minimize the escape energy. One must of course do this for each element of the attractor. This is not possible for the chaotic orbits but on these orbits the escape path with minimum energy always starts with  $x_0 = 0$  since  $x_1$  is the maximal point in

the orbit and  $x_2$  is the point in the orbit closest to  $x^*$ . The solid line denotes the minimum escape energy as determined numerically from Eq. (7).

We have tested these predictions with a Monte Carlo simulation. We simply iterate Eq. (2) starting at randomly selected points on the attractor. It is essential to use a Gaussian distribution for the random variables since the theory above is based on the statistics of Gaussian random numbers. Two uniformly distributed random numbers,  $u_1$  and  $u_2$ , on the interval (0,1) are used to generate the variable  $s$ :

$$s = (2u_1 - 1)^2 + (2u_2 - 1)^2;$$

if  $s \geq 1$  then two new variables  $u_1$  and  $u_2$  are generated. We then generate Gaussian random number  $r$  with zero mean and unit variance<sup>21</sup> by the formula

$$r = (2u_1 - 1)[ -2 \ln(s)/s ] .$$

The uniformly distributed random numbers are generated by a feedback shift-register technique.<sup>22</sup> The noise terms  $\xi_n$  are given by  $\xi_n = (\Gamma)^{1/2} r_n$ .

The initial point in each orbit is a randomly selected element of the attractor. The iteration of (2) continues for  $\tau$  iterations until the orbit leaves the basin of the attractor,  $|x_\tau| > |x^*|$ . An average of  $\ln(\tau)$  is kept for each value of the noise temperature  $\Gamma$ . (We use an average over  $\ln(\tau)$  since  $\tau$  is log-normally distributed.) One hundred different paths are used for each value of  $a$  and  $\Gamma$ . The function  $\langle \ln(\tau) \rangle$  is fit to an equation of the form  $\langle \ln(\tau) \rangle = \ln(\tau_0) + E_0/\Gamma$ . Only points with  $\tau \gg \tau_0$  are used in the fits since Eq. (1) is valid only for  $\Gamma \ll E_0$ . In no case are orbits with average escape time  $\tau < 400$  used in the fits. The maximum escape time used is  $\tau = 50\,000$ . The results are shown in Fig. 3. The minimum escape en-

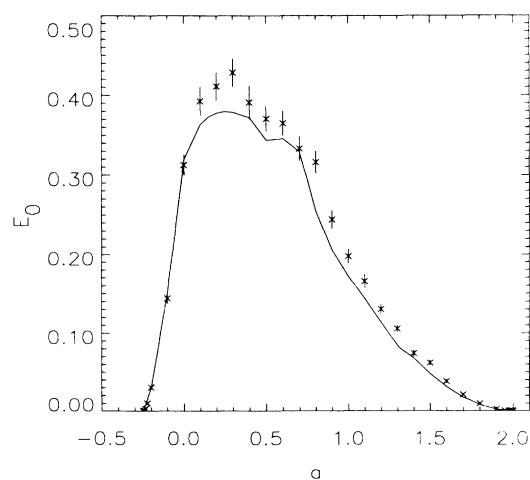


FIG. 3. The minimum noise energy  $E_0$  as a function of the control parameter  $a$ . The minimum noise energy vanishes at the tangent bifurcation ( $a = a_t = -\frac{1}{4}$ ) and at the crisis ( $a = a_c = 2$ ). The line is the theory and the data points are the results of the Monte Carlo simulation.

ergy vanishes as  $a \rightarrow a_t$  and  $a \rightarrow a_c$ . The point of maximal noise stability is approximately in the middle of the one-cycle region (however this is not near the superstable point at  $a=0$ ). The points with error bars are the results of the Monte Carlo simulations. The line is the theoretical minimum escape energy as determined analytically [Eqs. (16) and (20) near the endpoints of the attractor] and numerically for the remainder of the attracting range. The shape of the minimum escape energy curve is qualitatively similar to minimum escape energy in the rf-driven Josephson equation (Fig. 5 in Refs. 1 and 2). The escape energy from the rf-driven Josephson equation peaks in the middle of the one-cycle region, tends to zero rapidly at the tangent bifurcation and the crisis point. The theoretical curve in Fig. 3 always lies on or below the Monte Carlo values. This can be explained since there can be a large number of escape paths with escape energies close to but above the minimum escape energy path. These paths are sampled significantly unless the noise temperature is much smaller than the energy gap between the minimum escape energy and the escape energy of the other paths.

It is useful to test the exact results of the theory carefully near the tangent bifurcation and the crisis point. These results are shown in Figs. 4(a) and 4(b). The lines are the theory [Eqs. (16) and (20) with no adjustable parameters] and the data are the Monte Carlo results. The statistical errors are smaller than the data points. The theory is extremely accurate near the tangent bifurcation. Near the crisis point the theory slightly underestimates the minimum escape energy. This appears to be due to the strong divergence of the time between attempts near the crisis since the agreement improves when points with shorter escape times are removed from the fit.

Kautz observed that the time between attempts  $\tau_0$  in the rf-driven Josephson equation appears to diverge at the tangent bifurcation and the crisis point. To compare with this work, a plot of  $\log_{10}(\tau_0)$  versus  $a$  is shown in Fig. 5. Note that  $\tau_0$  appears to diverge at both the tangent bifurcation and the crisis point. The minimum in  $\tau_0$  appears to be close to the superstable fixed point of the one-cycle in agreement with Kautz's results<sup>1,2</sup> (see Fig. 6 in Ref. 1 and Fig. 5 in Ref. 2). Figures 6(a) and 6(b) show fits to power laws for the divergence of  $\tau_0$  near the tangent bifurcation and crisis point. Near the tangent bifurcation the divergence of the attempt time is consistent with a power-law dependence on  $a - a_t$ ,  $\tau_0 \sim (a - a_t)^{-0.62 \pm 0.10}$ . Kautz's exponent<sup>2</sup> for the resistively shunted Josephson equation is  $-0.5$ . Near the crisis we find that  $\tau_0 \sim (a_c - a)^{-0.42 \pm 0.15}$  in disagreement with Kautz's exponents<sup>1,2</sup> of  $-1.4$  and  $-0.8$ . Unfortunately, the method of minimum escape energy is not very helpful in resolving this discrepancy because the attempt rate is a difficult quantity to calculate within the formalism. It involves enumerating the number of paths with escape energy near the minimum escape energy. A Fokker-Planck approach would probably be more helpful for resolving this point.

We can now address the question of the manner in which the escape energy depends on the details of the mapping  $f(x)$ . If the logistic mapping is changed merely

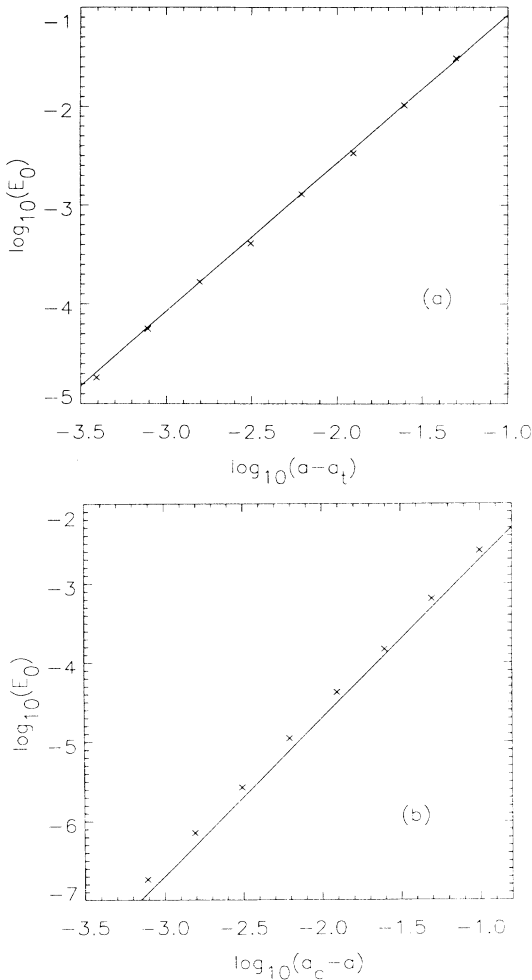


FIG. 4. A comparison of theory and Monte Carlo results (a) near the tangent bifurcation and (b) near the crisis. The lines are the theoretical predictions (16) and (20) with no adjustable parameters.

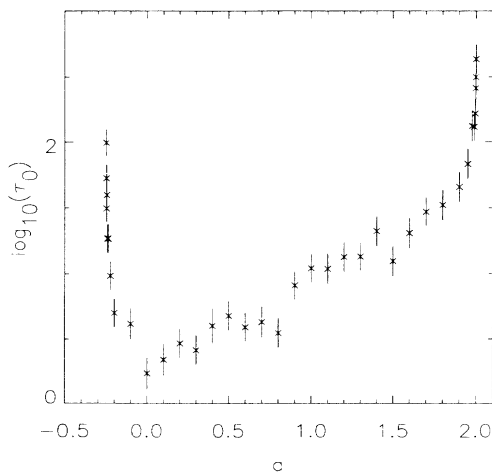


FIG. 5. The logarithm of the attempt time vs the control parameter. Note that  $\tau_0$  appears to diverge near the tangent bifurcation and the crisis, and that  $\tau_0$  is smallest near the superstable one-cycle ( $a=0.0$ ).

by a rescaling  $x_n \rightarrow y_n = \alpha x_n$ , the escape energy is rescaled by  $E_0 \rightarrow \alpha^2 E_0$ . For unimodal maps with quadratic maxima one would then expect that the escape energy would approximately scale with the square of the  $x$  distance between the maximum and the unstable fixed point  $x^*$ . This was checked by a Monte Carlo simulation of the escape from the superstable three-cycle of the logistic map. The mapping function is taken to be  $F(x) = f(f(f(x)))$  and  $a$  is chosen so as to give a superstable three-cycle ( $a = 1.754877666$ ). The noise is added only when the trajectory returns to the portion of the attractor which straddles  $x=0$ . Escape is defined as the number of iterations taken for the trajectory to lose three-cycle phase coherence. The unstable fixed point of  $F(x)$  near the origin is  $x^* = 0.10965$ . One would then expect the escape energy to be  $E_0 \approx (0.10965)^2 (0.31909) = 3.84 \times 10^{-3}$ , where 0.31909 is

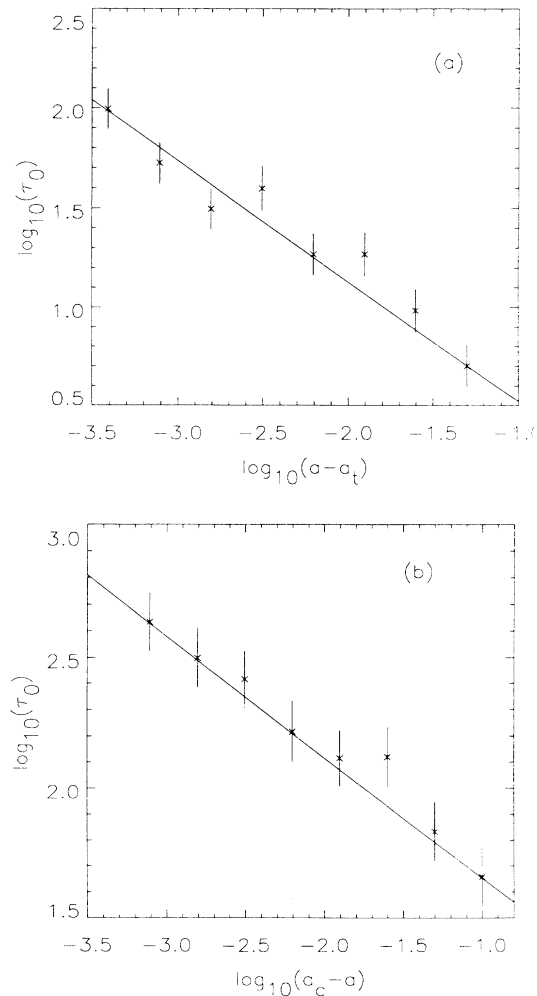


FIG. 6. The logarithm of the escape time  $\tau_0$  vs (a) the logarithm of  $a - a_t$  and (b) the logarithm of  $a_c - a$ . The slopes of these lines are the power-law divergence exponent for  $\tau_0$  at these two points. The slope in (a) is  $-0.62 \pm 0.10$  and the slope in (b) is  $-0.42 \pm 0.15$ .

the minimum escape energy for the superstable one-cycle. From the Monte Carlo simulation we found  $E_0 = (3.50 \pm 0.16) \times 10^{-3}$  in reasonable agreement with the prediction.

We also investigated the three-cycle when the noise is added at every step rather than every third step. The effect of the noise is multiplied because of the combined effect of the noise added at each step of the three-cycle. For example,

$$x_3 = x_0 + \xi_0 f'(\bar{x}_1) f'(\bar{x}_2) + \xi_1 f'(\bar{x}_2) + \xi_2 + O(\xi^2), \quad (21)$$

where

$$\begin{aligned} \bar{x}_1 &= f(x_0), \\ \bar{x}_2 &= f(\bar{x}_1), \\ x_0 &= f(\bar{x}_2). \end{aligned} \quad (22)$$

The effective noise is

$$\xi^{\text{eff}} = \xi_0 f'(\bar{x}_1) f'(\bar{x}_2) + \xi_1 f'(\bar{x}_2) + \xi_2 + O(\xi^2), \quad (23)$$

and the effective noise temperature is

$$\begin{aligned} \Gamma^{\text{eff}} &= \langle (\xi^{\text{eff}})^2 \rangle \\ &= \Gamma \{ 1 + [f'(\bar{x}_2)]^2 + [f'(\bar{x}_1) f'(\bar{x}_2)]^2 \}. \end{aligned} \quad (24)$$

For the superstable three-cycle the effective noise temperature is

$$\Gamma^{\text{eff}} = 99.8 \Gamma, \quad (25)$$

so that the minimum escape energy should be approximately

$$E_0 \approx \frac{(0.10965)^2 (0.31909)}{(99.8)} = 3.84 \times 10^{-5}. \quad (26)$$

The escape energy found from the Monte Carlo simulation in which noise was added every step was  $E_0 = (3.96 \pm 0.19) \times 10^{-5}$ . A numerical calculation of the minimum escape energy based on Eqs. (7) and (12) gives  $E_0 = 4.13 \times 10^{-5}$ .

In conclusion, we calculated the minimum escape energy for noise-induced escape from the attractor of the logistic map. Near a tangent bifurcation the minimum escape energy is proportional to  $(a - a_t)^{3/2}$  and near an internal crisis the escape energy is proportional to  $(a_c - a)^2$ . We conjecture that these exponents are universal. The point of minimum escape energy is largest roughly in the center of the one-cycle region and the attempt time diverges at both the tangent bifurcation and the crisis.

I would like to thank Dick Kautz for introducing me to this subject and for his helpful comments regarding this manuscript, and Peter Grassberger for sharing his results with me prior to publication. Some of the calculations described were performed on computers at the John von Neumann Computer Center and funded by the National Allocation Committee of the National Science Foundation under Grant No. NAC-1242.

<sup>1</sup>R. L. Kautz, in *Structure, Coherence and Chaos in Dynamical Systems*, edited by Peter L. Christensen and Robert D. Parmentier (Manchester University Press, New York, 1989).  
<sup>2</sup>R. L. Kautz, *J. Appl. Phys.* **62**, 198 (1987).  
<sup>3</sup>R. L. Kautz, *Phys. Lett. A* **125**, 315 (1987).  
<sup>4</sup>R. L. Kautz, *Phys. Rev. A* **38**, 2066 (1988).  
<sup>5</sup>M. I. Freidlin and A. D. Wentzell, *Random Perturbations of Dynamical Systems* (Springer-Verlag, New York, 1984).  
<sup>6</sup>N. G. Van Kampen, *Stochastic Processes in Physics and Chemistry* (North-Holland, New York, 1981), and references therein.  
<sup>7</sup>D. E. McCumber, *J. Appl. Phys.* **39**, 3113 (1968).  
<sup>8</sup>W. C. Stewart, *Appl. Phys. Lett.* **12**, 277 (1968).  
<sup>9</sup>B. A. Huberman, J. P. Crutchfield, and N. Packard, *Appl. Phys. Lett.* **37**, 750 (1980); E. Ben Jacob, Y. Braiman, and R. Shainsky, *ibid.* **38**, 822 (1981); D. D'Humieres, M. R. Beasley, B. A. Huberman, and A. Libchaber, *Phys. Rev. A* **26**, 3483 (1982).  
<sup>10</sup>R. L. Kautz, *J. Appl. Phys.* **52**, 6241 (1981).  
<sup>11</sup>R. M. May, *Nature (London)* **261**, 459 (1976).

<sup>12</sup>P. Collet and J.-P. Eckmann, *Iterated Maps on the Interval as Dynamical Systems* (Birkhauser, Boston, 1980).  
<sup>13</sup>M. J. Feigenbaum, *J. Stat. Phys.* **19**, 25 (1978); *Los Alamos Science* **1**, 4 (1980).  
<sup>14</sup>P. Mannville and Y. Pomeau, *Phys. Lett.* **75A**, 1 (1979); *Commun. Math. Phys.* **74**, 189 (1980).  
<sup>15</sup>J. P. Eckmann, L. Thomas, and P. Wittwer, *J. Phys. A* **14**, 3153 (1981); J. P. Hirsh, B. A. Hubermann, and D. J. Scalapino, *Phys. Rev. A* **25**, 519 (1982).  
<sup>16</sup>C. Grebogi, E. Ott, and J. A. Yorke, *Physica D* **7**, 181 (1983).  
<sup>17</sup>J. P. Crutchfield, J. D. Farmer, and B. A. Hubermann, *Phys. Rep.* **92**, 45 (1982).  
<sup>18</sup>F. T. Arecchi, R. Badii, and A. Politi, *Phys. Lett.* **103A**, 3 (1984).  
<sup>19</sup>S. Takesue and K. Kaneko, *Prog. Theor. Phys.* **71**, 35 (1984).  
<sup>20</sup>P. Grassberger (unpublished).  
<sup>21</sup>Donald E. Knuth, *The Art of Computer Programming* (Addison-Wesley, Reading, MA, 1969), Vol. 2.  
<sup>22</sup>S. Kirkpatrick and E. Stoll, *J. Comput. Phys.* **40**, 517 (1981).